Adaptive optoelectronic camouflage systems with designs inspired by cephalopod skins

Cunjiang Yu[a], Yuhang Li[b,c], Xun Zhang[d], Xian Huang[d], Viktor Malyarchuk[d], Shuodao Wang[d], Yan Shi[b,e], Li Gao[d], Yewang Su[b], Yihui Zhang[b], Hangxun Xu[f], Roger T. Hanlon[g,h], Yonggang Huang[b], and John A. Rogers[d,i,1]

[a]Department of Mechanical Engineering, Department of Electrical and Computer Engineering, University of Houston, Houston, TX 77204; [b]Department of Civil and Environmental Engineering, Department of Mechanical Engineering, Center for Engineering and Health, and Skin Disease Research Center, Northwestern University, Evanston, IL 60208; [c]The Solid Mechanics Research Center, Beihang University, Beijing 100191, China; [d]Department of Materials Science and Engineering, University of Illinois at Urbana–Champaign, Urbana, IL 61801; [e]State Key Laboratory of Mechanics and Control of Mechanical Structures, Nanjing University of Aeronautics and Astronautics, Nanjing 210016, China; [f]Department of Polymer Science and Engineering, Chinese Academy of Sciences Key Laboratory of Soft Matter Chemistry, University of Science and Technology of China, Hefei 230026, China; [g]Marine Biological Laboratory, Woods Hole, MA 02543; [h]Department of Ecology and Evolutionary Biology, Brown University, Providence, RI 02912; and [i]Department of Electrical and Computer Engineering, Department of Chemistry, Department of Mechanical Science and Engineering, Frederick Seitz Materials Research Laboratory, and Beckman Institute for Advanced Science and Technology, University of Illinois at Urbana–Champaign, Urbana, IL 61801

Edited by David A. Weitz, Harvard University, Cambridge, MA, and approved July 30, 2014 (received for review June 5, 2014)

Octopus, squid, cuttlefish, and other cephalopods exhibit exceptional capabilities for visually adapting to or differentiating from the coloration and texture of their surroundings, for the purpose of concealment, communication, predation, and reproduction. Longstanding interest in and emerging understanding of the underlying ultrastructure, physiological control, and photonic interactions has recently led to efforts in the construction of artificial systems that have key attributes found in the skins of these organisms. Despite several promising options in active materials for mimicking biological color tuning, existing routes to integrated systems do not include critical capabilities in distributed sensing and actuation. Research described here represents progress in this direction, demonstrated through the construction, experimental study, and computational modeling of materials, device elements, and integration schemes for cephalopod-inspired flexible sheets that can autonomously sense and adapt to the coloration of their surroundings. These systems combine high-performance, multiplexed arrays of actuators and photodetectors in laminated, multilayer configurations on flexible substrates, with overlaid arrangements of pixelated, color-changing elements. The concepts provide realistic routes to thin sheets that can be conformally wrapped onto solid objects to modulate their visual appearance, with potential relevance to consumer, industrial, and military applications.

flexible electronics | metachrosis | thermochromic

Recently established understanding of many of the key organ and cellular level mechanisms of cephalopod metachrosis (1–5) creates opportunities for the development of engineered systems that adopt similar principles. Here, critical capabilities in distributed sensing and actuation (6–9) must be coupled with elements that provide tunable coloration, such as the thermochromic systems reported here or alternatives such as cholesteric liquid crystals (10–13), electrokinetic and electrofluidic structures (14, 15), or colloidal crystals (16–19). Although interactive displays that incorporate distributed sensors for advanced touch interfaces (20–22) might have some relevance, such capabilities have not been explored in flexible systems or in designs that enable adaptive camouflage. The results reported here show that advances in heterogeneous integration and high-performance flexible/stretchable electronics provide a solution to these critical subsystems when exploited in thin multilayer, multifunctional assemblies. The findings encompass a complete set of materials, components, and integration schemes that enable adaptive optoelectronic camouflage sheets with designs that capture key features and functional capabilities of the skins of cephalopods. These systems combine semiconductor actuators, switching components, and light sensors with inorganic reflectors and organic color-changing materials in a way that allows autonomous matching to background coloration, through the well-known, separate working principles of each component. The multilayer configuration and the lamination processes used for assembly, along with the photopatternable thermochromic materials, are key to realization of these systems. Demonstration devices capable of producing black-and-white patterns that spontaneously match those of the surroundings, without user input or external measurement, involve multilayer architectures and ultrathin sheets of monocrystalline silicon in arrays of components for controlled, local Joule heating, photodetection, and two levels of matrix addressing, combined with metallic diffuse reflectors and simple thermochromic materials, all on soft, flexible substrates. Systematic experimental, computational, and analytical studies of the optical, electrical, thermal, and mechanical properties reveal the fundamental aspects of operation, and also provide quantitative design guidelines that are applicable to future embodiments.

The skin of a cephalopod enables rapid, patterned physiological color change, or metachrosis, in a thin three-layered system (2, 23–25). The topmost layer is pigmentary coloration: chromatophore organs that retract or expand rapidly by direct control of muscles that are in turn controlled by nerves originating in the brain. This physiological on/off speed change

Significance

Artificial systems that replicate functional attributes of the skins of cephalopods could offer capabilities in visual appearance modulation with potential utility in consumer, industrial, and military applications. Here we demonstrate a complete set of materials, components, fabrication approaches, integration schemes, bioinspired designs, and coordinated operational modes for adaptive optoelectronic camouflage sheets. These devices are capable of producing black-and-white patterns that spontaneously match those of the surroundings, without user input or external measurement. Systematic experimental, computational, and analytical studies of the optical, electrical, thermal, and mechanical properties reveal the fundamental aspects of operation and also provide quantitative design guidelines that are applicable to future embodiments.

Author contributions: C.Y. and J.A.R. designed research; C.Y., Y.L., X.Z., X.H., V.M., S.W., Y. Shi, L.G., Y. Su, Y.Z., H.X., Y.H., and J.A.R. performed research; C.Y., Y.L., Y. Su, Y.Z., Y.H., and J.A.R. analyzed data; and C.Y., Y.L., Y. Shi, Y. Su, R.T.H., Y.H., and J.A.R. wrote the paper.

The authors declare no conflict of interest.

This article is a PNAS Direct Submission.

[1]To whom correspondence should be addressed. Email: jrogers@illinois.edu.

This article contains supporting information online at www.pnas.org/lookup/suppl/doi:10.1073/pnas.1410494111/-/DCSupplemental.

ranges from *ca.* 250 to 750 ms. The middle and bottom layers are composed of structural coloration components. The middle layer comprises iridophore cells that can reflect all colors depending on angle of view; some are passive cells and others are physiologically controlled by a slower system: They can be turned on/off in 2–20 s (depending on species, or different cell types on different parts of the body). The bottom layer comprises leucophores (i.e., "white cells") that are entirely passive (i.e., no physiological control; they are always "on"). This layer diffuses white in all directions (25) and can act as a bright backdrop

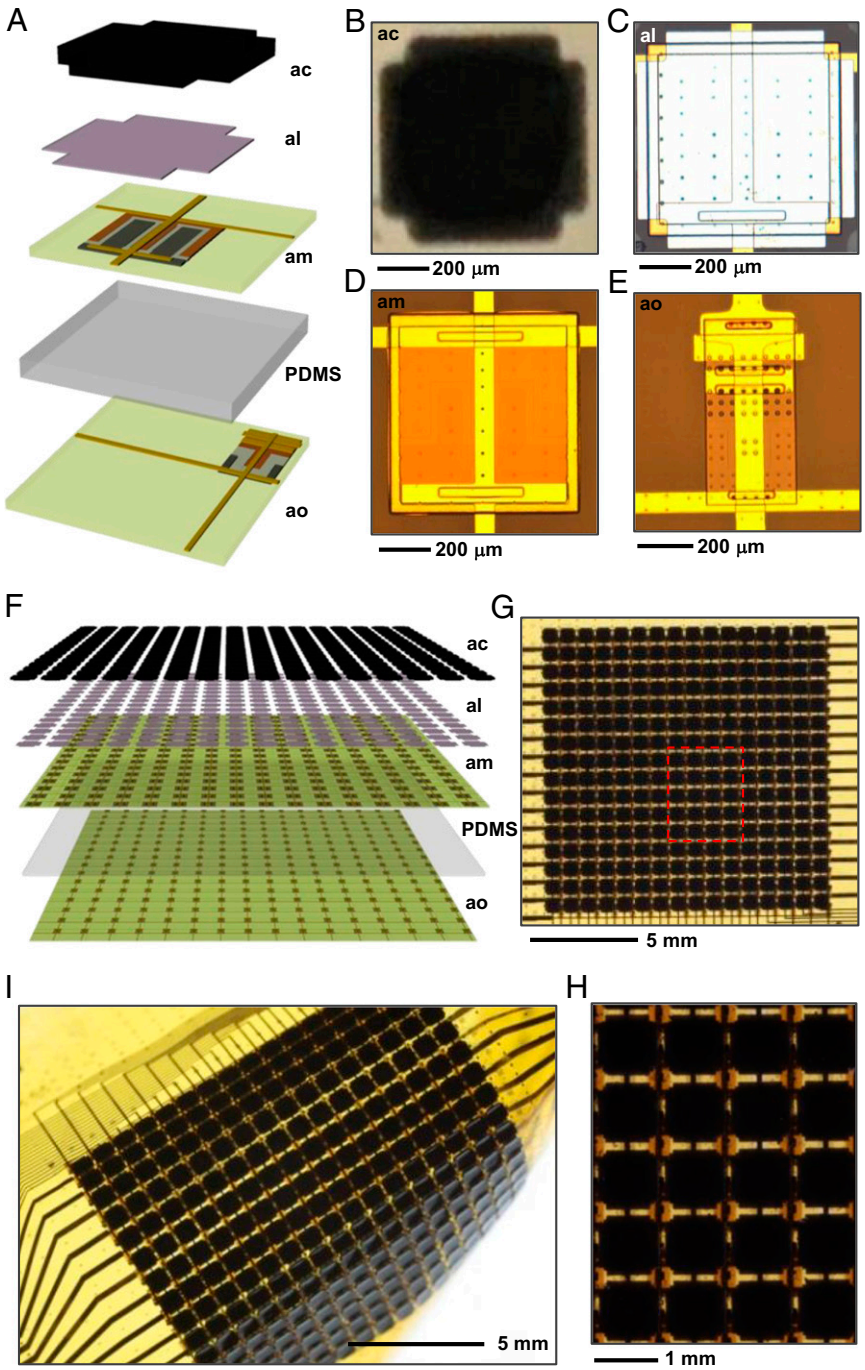

Fig. 1. Schematic illustrations and images of adaptive camouflage systems that incorporate essential design features found in the skins of cephalopods. (*A*) Exploded view illustration of a single unit cell that highlights the different components and the multilayer architecture. The first and second layers from the top correspond to the leucodye composite (artificial chromatophore; ac) and the Ag white reflective background (artificial leucodye; al). The third layer supports an ultrathin silicon diode for actuation, with a role analogous to that of the muscle fibers that modulate the cephalopod's chromatophore (artificial muscle; am). The bottom layer, separated from the third layer by PDMS, provides distributed, multiplexed photodetection, similar to a postulated function of opsin proteins found throughout the cephalopod skin (artificial opsin; ao). (*B*) Optical image of a thermochromic equivalent to a chromatophore. (*C*) Optical micrograph of the Ag layer and the silicon diode. (*D*) Optical image of the diode. (*E*) Optical image of a photodiode and an associated blocking diode for multiplexing. (*F*) Exploded view of illustration of a 16 × 16 array of interconnected unit cells in a full, adaptive camouflage skin. (*G*) Top view image of such a device. (*H*) Image of the region highlighted by the red box in *G*. (*I*) Image of a device in a bent configuration.

against which expanded pigmentary chromatophores are viewed; this provides one way in which contrast of the pattern can be controlled (i.e., darkly pigmented chromatophores next to bright white reflective elements).

The central control of skin patterning resides in the eyes, which, together with the central and peripheral nervous system, sense the visual background and route control signals throughout the skin to produce a coordinated pattern for communication or camouflage. In addition, the skin contains molecules known as opsins, which are known to be photosensitive in the retina and are thought to be photosensitive in the skin as well. They are hypothesized to play a role in distributed light sensing and control in the periphery (26), thus potentially adding a noncentralized component for skin patterning that enables sensing and actuation independent of the brain.

One of the most important features of cephalopod skin—one that provides maximum optical diversity of appearances—is the coordinated action of (*i*) chromatophores, (*ii*) iridophores, (*iii*) leucophores, (*iv*) muscles, (*v*) central ocular organs, and (*vi*) distributed opsins (2, 23–25). The work described here demonstrates pixelated devices that include analogs to each of these key elements, except for the second and fifth, which can be easily incorporated with known photonic materials and conventional digital imagers.

Results

Fig. 1*A* presents a schematic illustration of a unit cell; the multilayer stack includes, from top to bottom, a color-changing element (analogous to a chromatophore) on top of a white reflective surface (analogous to a leucophore), an actuator (analogous to the muscles that control the chromatophore), and a light sensor (analogous to a functional unit involving opsins), all on a flexible plastic support. Optical images illustrate the materials and device structures used for each of these components: microencapsulated thermochromic dye embedded in a photopatternable polymer matrix (Fig. 1*B*) to define the color, a thin layer of silver (Ag) to create a bright white background (Fig. 1*C*), an ultrathin silicon (Si) diode to provide multiplexed Joule heating for control over the optical properties of the dye (Fig. 1*D*), and an ultrathin Si photodiode and blocking diode, also configured for multiplexing, to yield a control signal (Fig. 1*E*). A complete system consists of a 16 × 16 array of such unit cells, in the form of a flexible skin (1.4 cm × 1.4 cm), as illustrated schematically in Fig. 1*F* and in the images of Fig. 1 *G* and *H*. The thin geometries of the active components and the compliance of the polydimethylsiloxane (PDMS; 100 μm thick; ~2 MPa modulus) substrate lead to high levels of mechanical flexibility (Fig. 1*I*).

The artificial chromatophores incorporate a thin layer of microencapsulated leucodye (black 47C, LCR Hallcrest) embedded in a photosensitive transparent polymer (SU-8 50, Microchem). The dye is based on a fluoran chemistry that reversibly converts from open (colored) to closed (colorless) form lactone rings upon temperature cycling below and above 47 °C, respectively. This composite combines abilities for color modulation via the leucodye (27–29) with photopatterning via the transparent polymer matrix. An example of a black (transparent) slurry of this composite at 22 °C (47 °C) is shown in *SI Appendix*, Fig. S1 *A* and *B*. Crosslinking by patterned exposure to UV light allows unexposed regions to be washed away, thereby yielding pixelated patterns (thicknesses of ~65 μm and edge resolution of 10 μm) such as those shown in Fig. 1*B*. The notched corners create openings for light sensing by photodetectors located at these positions. Details appear in *SI Appendix*, including scanning electron microscope images in *SI Appendix*, Fig. S1.

The results from an artificial chromatophore of this type at 22 °C and 47 °C are shown in *SI Appendix*, Fig. S1 *E* and *F*. Here, a thin layer of Ag, also patterned into a pixelated geometry, serves as an artificial leucophore to provide a bright white reflective background. Corresponding spectral reflectance properties appear in Fig. 2*A* as a function of temperature. The reflectance can be further improved by use of strongly scattering materials (e.g., titania nanoparticles) and/or thermochromic materials with improved transmittance in their transparent state.

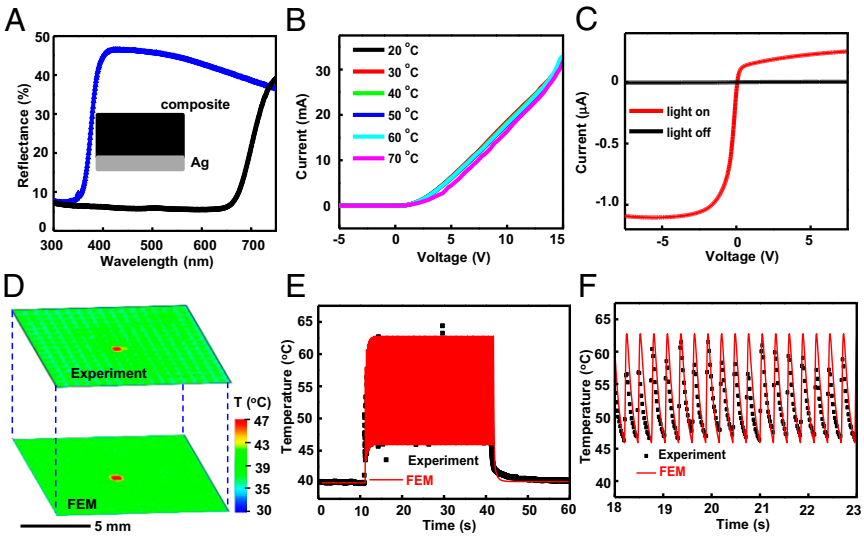

Fig. 2. Photodetection and color switching. (*A*) Optical reflectance measured throughout the visible range and at normal incidence from a layer of a thermochromic composite on a white Ag film, at 20 °C (black) and 47 °C (white). (*Inset*) The cross section of the structure. (*B*) I-V characteristics of a multiplexed diode for actuation, measured at temperatures between 20 °C and 70 °C, with an increment of 10 °C. (*C*) I-V characteristics of a multiplexed photodetector measured while under white light illumination (light on, red) and in the dark (light off, black). (*D*) Measured (IR image; top) and computed (3D FEM; bottom) distributions of temperature associated with a device during multiplexed actuation of a single unit cell located in the center. (*E*) Time-dependent variations in temperature at the center of a unit cell during multiplexed actuation that begins at ~11 s and ends at ~41 s. The black dots are experimental data extracted from movies recorded using an IR camera. The red curve represents FEM results. (*F*) Experimental and FEM results for times between ~18 s and ~23 s. The minimum and maximum temperatures are ~47 °C and ~62 °C, respectively.

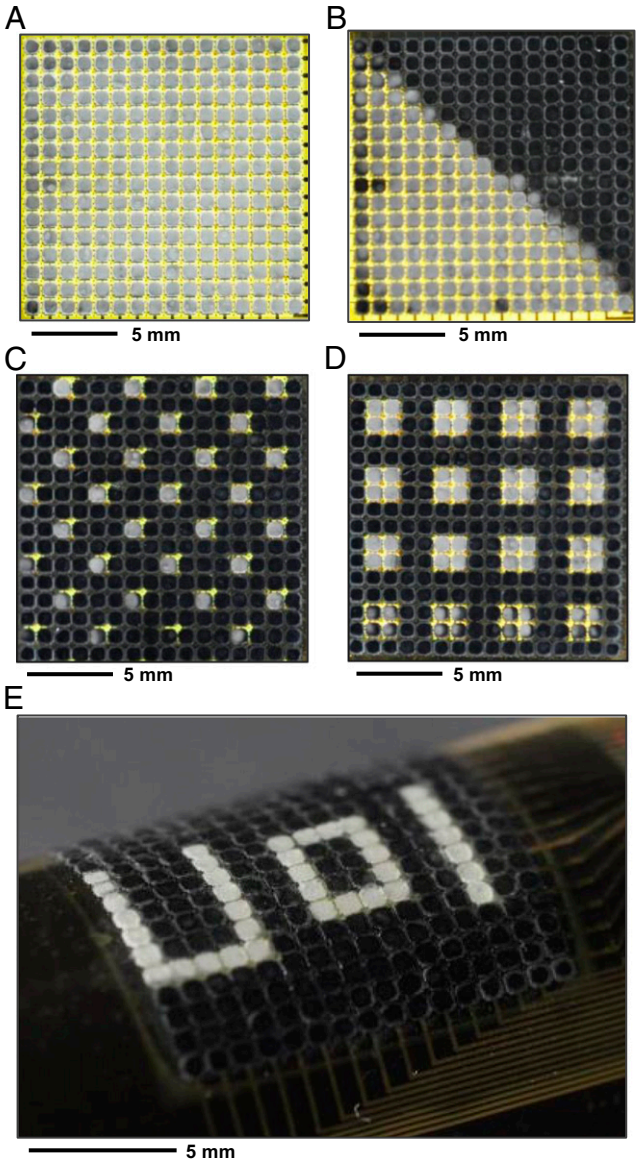

Fig. 3. Illustration of metachrosis for several different static patterns. Top view image of the device in a uniform geometry (*A*), in a triangular pattern (*B*), and in an array of small (*C*) and large (*D*) squares. (*E*) Image of a device in operation while bent, while showing the text pattern "U o I".

This color changing strategy offers viewing-angle-independent appearance and a simple, thermal switching mechanism, suitable for present demonstration purposes. The high thermal conductivity of the Ag layer is important for this latter feature, as described subsequently.

Selective actuation of these photodefined chromatophores/leucophores yields programmable patterns of black and white. An array of ultrathin (total thickness ~10 μm; bending stiffness per length ~1.7 μN) Si diodes (single crystal Si 640 × 640 μm^2 in area, 1.25 μm thick) provides local heating for this purpose, with multiplexed addressing (*SI Appendix*, Fig. S2). Details of the fabrication and optical images of representative devices appear in *SI Appendix*, Figs. S3, S4, and S2*C*, respectively. The yields are >95%. Fig. 2*B* presents the current-voltage (I-V) characteristics of a typical device (forward voltage ~0.7 V; current ~190 mA at a forward bias of 10.5 V). The properties are independent of temperature over this range, thereby ensuring stable behavior in all relevant operating modes presented here. Multiplexed addressing involves application of power in a pulsed mode, with row/column scanning. The designs of the external electronics for this purpose are summarized in *SI Appendix*, Figs. S5 and S6. The ability to localize heating to a single unit cell in this manner is demonstrated in *SI Appendix*, Fig. S2*D*.

Distributed sensing of background patterns is achieved via artificial opsins that consist of photodiodes and multiplexing switches. The materials and fabrication schemes for these components are similar to those of the Joule heating elements described above. (Details appear in *SI Appendix*.) The responses of the photodetectors define the pattern of thermal actuation and, therefore, the resulting patterns of coloration. As illustrated in Fig. 1*E* and *SI Appendix*, Fig. S7 *A* and *B*, each unit cell includes a photodiode and a multiplexing (blocking) diode connected in a back-to-back fashion. These devices are positioned at the notches in the patterned chromatophore/leucophore pixels to allow exposure to light incident on the system from above or below. The blocking diode incorporates an opaque coating to eliminate its sensitivity to light. The I-V curves of the photodetector in dark and light conditions appear in Fig. 2*C*, where the dark current is ~1 nA and the photocurrent is ~1 μA. The yields are ~100%. A digital image that results from patterned illumination appears in *SI Appendix*, Fig. S8 *A* and *B*. A binarized intensity distribution derived from such an image serves as a control signal to establish closed-loop operation of the entire system. The actuation and sensing layers have excellent flexibility (*SI Appendix*, Figs. S4*D* and S7*C*) due to their thin construction. No delamination occurs even when the integrated device was bent to a radius of 2 mm. Finite element modeling (FEM) results for bending to this degree appear in *SI Appendix*, Fig. S12*A*. The same geometry allows separate fabrication of these layers and subsequent lamination of them on top of one another to form a complete system (*SI Appendix*, Fig. S9). The lamination process occurs at the wafer scale, with the potential for use over larger areas with proper tooling and alignment procedures. This type of integration allows separate fabrication of the various subsystems, thereby improving the overall device yields, to levels of >95%. Images of the device before and after integrating the Ag layers are shown in *SI Appendix*, Fig. S10 *A* and *B*. Thin flexible cables based on anisotropic conductive films bond to electrode pads at the periphery for electrical connection to external power supply and analysis hardware, as in *SI Appendix*, Fig. S11.

Multiplexed photodetection and coordinated actuation are central to the overall operation. Responses of the diodes under pulsed mode voltages between 5.5 V and 12.5 V yield insights into the mechanisms of heating and thermal diffusion. Measurements under these conditions involve digital image capture of color changes in the chromatophore, simultaneously with temperature evaluation using an infrared (IR) camera (A655SC, FLIR Systems, Inc.). The minimum operating voltage is defined by initiation of color change at the location of the targeted pixel; the maximum is defined by onset of change in adjacent pixels, via thermal diffusion. As shown in *SI Appendix*, Figs. S13 and S14, typical minimum and maximum voltages are ~10.5 V and ~11.5 V, respectively. All system tests reported here used values near the minimum. Fig. 2*D* illustrates measured (top) and computed (bottom) distributions of temperature during operation of a single, isolated pixel. The multiplexing scheme naturally leads to fluctuations in temperature about a baseline level, as shown in the experimental (black dots) and 3D FEM results (red lines) of Fig. 2 *E* and *F*, and *SI Appendix*, Fig. S15. Here, the applied power begins and ends at 11 s and 41 s, respectively. The pulses have a duration of $t_0 = 17.5$ ms and a period of $T = 280$ ms. The color changes from white to black after ~1 s, corresponding to four pulses. Results of *SI Appendix*, Fig. S15*B*, indicate that the temperature increases sharply and then fluctuates between 47 °C and 60 °C, after stabilization. A key finding is that changes in

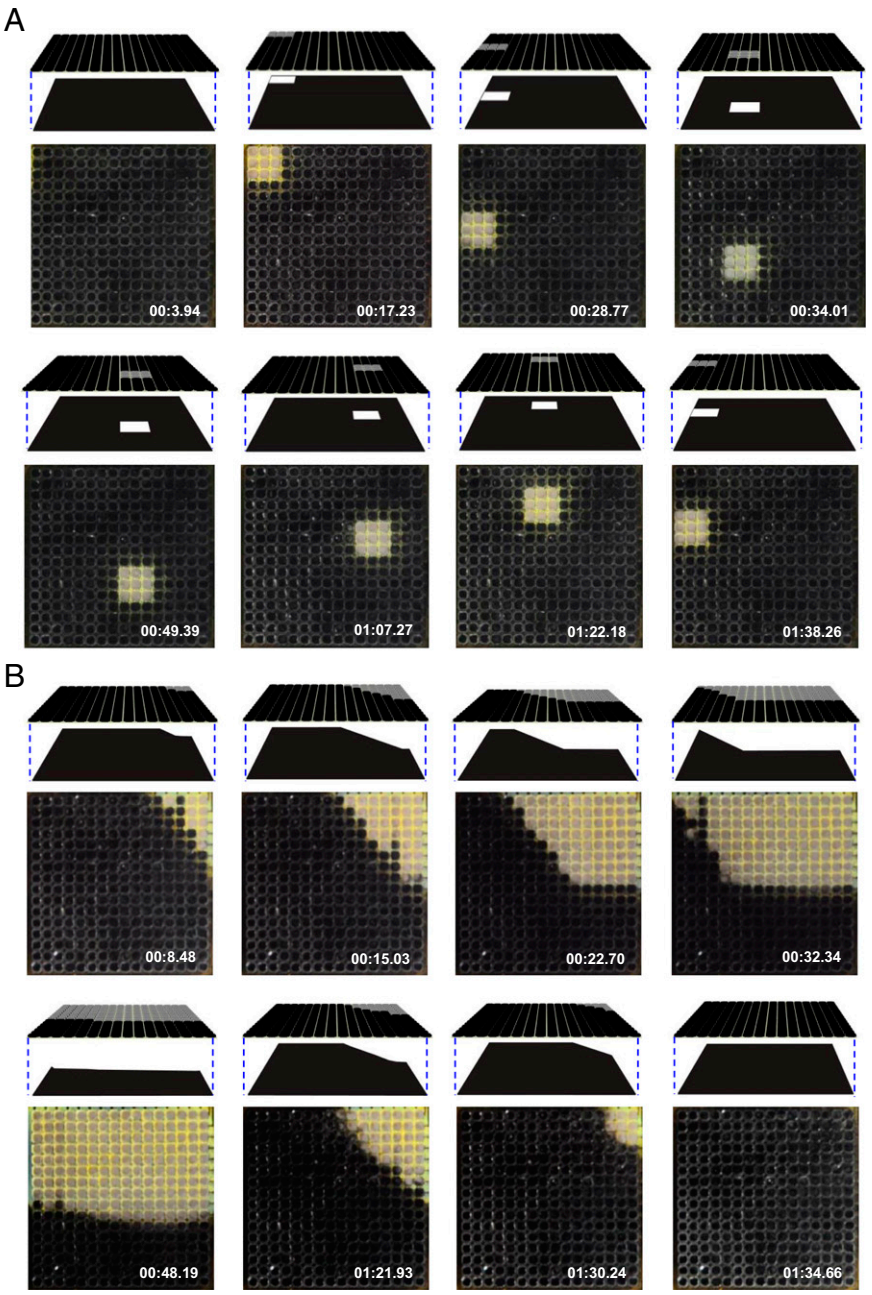

Fig. 4. Two demonstrations of autonomous, dynamic metachrosis. (*A*) Sequence of images extracted from a movie (time stamp in the lower right) that demonstrates adaptive pattern matching to a continuously changing background, created in this case by moving a mask that allows passage of light through a square region. At the top are angled view schematic illustrations of the experiment (top: device; bottom: pattern background). (*B*) Results similar to those in *A*, but obtained with a different mask geometry.

temperature remain confined largely to a single pixel, without significant diffusion to neighboring pixels (*SI Appendix*, Fig. S17). The lateral uniformity and pixel-level localization of the changes in temperature follow from (*i*) the high thermal conductivity of the Ag layer and its ability to facilitate thermal diffusion from the diode source (*SI Appendix*, Fig. S20) and (*ii*) the pixelated pattern of this material and the leucodye composite. The temperature (see *SI Appendix*, Fig. S18) is nearly constant throughout the depth of this composite (see *SI Appendix*, Fig. S19), due to its thin geometry. These collective features enable arbitrary pattern generation to a resolution set by the numbers of pixels and their sizes. An example of a pattern of the character "O" appears in Movie S1 (experimental results) and Movie S2 (modeling results).

Experimental procedures used to study camouflage capabilities in cuttlefish (2, 30–33) serve as a model for illustrating full function, i.e., metachrosis, of the systems. Here, a device rests on a patterned black-and-white background formed by passing white light through an amplitude mask from below. External control electronics automatically send signals to the actuators at locations where responses from associated photodetectors exceed a threshold. Fig. 3*A* shows a case in which all pixels turn white, consistent with the uniformly bright pattern of the background. Different static geometries, including triangles,

arrays of dots, and even random patterns, can be achieved, with either flat or curved configurations, as shown in Fig. 3 *B–E*.

Dynamic pattern recognition and matching are also possible, as illustrated in Fig. 4 *A* and *B*. In this case, changing the position of an amplitude mask that passes light only through a small square region leads to corresponding changes in the displayed patterns (Fig. 4*A*). In these images and others of Fig. 4, the top illustrations correspond to schematic, angled view renderings of the mask and the device; the images directly below are top views of the device. Movies S3 and S4 show additional details and examples. The metachrosis process occurs within 1 or 2 s in all cases, which is similar to neutrally controlled pattern change in cephalopods (2).

Discussion

These systems establish foundations in materials science and engineering design that address key challenges in distributed sensing, actuation, and control in adaptive camouflage. The sensors and actuators provide operation across the full visible spectrum and allow for electric-field– or current-induced switching, respectively. As a result, these ideas can be applied not only with simple thermochromic materials but also with more advanced alternatives that offer improved power efficiency, facile routes to color, and robust operation without sensitivity to environmental conditions. Furthermore, the overall architecture can accommodate integration of tunable analogs to iridophores, thereby providing a vehicle for future investigations. In all cases, compatibility with large-area electronics holds promise for scalable manufacturing. Ability to reproduce physical texture, as in many cephalopods (34), remains as an interesting and challenging topic for research.

Materials and Methods

Fabrication and Assembly. Detailed fabrication procedures for the various individual components of the system appear in *SI Appendix*. The assembly process involves a series of lamination processes. First, a slab of PDMS (Sylgard 184, Dow Corning) was used to retrieve an interconnected array of multiplexed silicon diodes after release from a glass substrate. Exposing a separate layer of PDMS (100 μm, on a glass substrate) to UV-induced ozone (BHK, Inc.) generated a hydroxyl-terminated surface for bonding via condensation reactions with similar chemistry associated with a layer SiO_2 blanket deposited onto the array. The Ag (thickness 300 nm) and the thermochromic composite (thickness ~65 μm) were lithographically patterned on top of the diode array. Alignment followed a scheme shown in *SI Appendix*, Fig. S10C. The resulting system, with the PDMS layer, was then peeled from the glass. Similar bonding processes enabled aligned integration of a separately fabricated multiplexed array of photodetectors onto the backside of the PDMS, through the use of modified mask aligner (MJB-3, Karl Suss) with alignment accuracy of 1 μm. Details appear in *SI Appendix*, Fabrication and assembling the complete system and Fig. S9.

Control and System Operation. The system consists of two sets of active components, i.e., sensors and actuators, each of which functions separately and at different multiplexed scanning speeds. Closed-loop operation involves (*i*) acquiring digital images based on the intensity distributions extracted from responses of the 16 × 16 array of photodetectors, (*ii*) binarizing the intensity distribution and storing the resulting data in a buffer, and (*iii*) reading the buffer and addressing the 16 × 16 array of actuators by column scanning to copy the pattern, in a repeating manner. The time to acquire an image is ~10 ms, much shorter than the pulse period for actuation (280 ms), thereby ensuring that the refresh rate of the image exceeds that of induced color change. Software development tools from LabVIEW 2012 provide all of the necessary means for implementation of the described operation.

ACKNOWLEDGMENTS. Jeff Grau is acknowledged for his help in preparing photomasks. The work on material design and device fabrication was supported by Office of Naval Research under Grant N00014-10-1-0989. C.Y. acknowledges the start-up funding support from the Department of Mechanical Engineering, Cullen College of Engineering, and the Division of Research at the University of Houston. R.T.H. also acknowledges partial support from Air Force Office of Scientific Research Grant FA9550–09–0346.

1. Mäthger LM, Denton EJ, Marshall NJ, Hanlon RT (2009) Mechanisms and behavioural functions of structural coloration in cephalopods. *J R Soc Interface* 6(Suppl 2): S149–S163.
2. Hanlon R (2007) Cephalopod dynamic camouflage. *Curr Biol* 17(11):R400–R404.
3. Hanlon RT, et al. (2009) Cephalopod dynamic camouflage: Bridging the continuum between background matching and disruptive coloration. *Philos Trans R Soc Lond B Biol Sci* 364(1516):429–437.
4. Messenger JB (2001) Cephalopod chromatophores: Neurobiology and natural history. *Biol Rev Camb Philos Soc* 76(4):473–528.
5. Hanlon RT (1982) The functional-organization of chromatophores and iridescent cells in the body patterning of *Loligo-plei* (Cephalopoda, Myopsida). *Malacologia* 23(1):89–119.
6. Manakasetthарn S, Taylor JA, Krupenkin TN (2011) Bio-inspired artificial iridophores based on capillary origami: Fabrication and device characterization. *Appl Phys Lett* 99(14):144102.
7. Morin SA, et al. (2012) Camouflage and display for soft machines. *Science* 337(6096): 828–832.
8. Rossiter J, Yap B, Conn A (2012) Biomimetic chromatophores for camouflage and soft active surfaces. *Bioinspir Biomim* 7(3):036009.
9. Phan L, et al. (2013) Reconfigurable infrared camouflage coatings from a cephalopod protein. *Adv Mater* 25(39):5621–5625.
10. Coles HJ, Pivnenko MN (2005) Liquid crystal 'blue phases' with a wide temperature range. *Nature* 436(7053):997–1000.
11. Kahn FJ (1970) Electric-field-induced color changes and pitch dilation in cholesteric liquid crystals. *Phys Rev Lett* 24(5):209–212.
12. Kikuchi H, Yokota M, Hisakado Y, Yang H, Kajiyama T (2002) Polymer-stabilized liquid crystal blue phases. *Nat Mater* 1(1):64–68.
13. Sackmann E (1971) Photochemically induced reversible color changes in cholesteric liquid crystals. *J Am Chem Soc* 93(25):7088–7090.
14. Comiskey B, Albert JD, Yoshizawa H, Jacobson J (1998) An electrophoretic ink for all-printed reflective electronic displays. *Nature* 394(6690):253–255.
15. Heikenfeld J, et al. (2009) Electrofluidic displays using Young–Laplace transposition of brilliant pigment dispersions. *Nat Photonics* 3(5):292–296.
16. Vukusic P, Sambles JR (2003) Photonic structures in biology. *Nature* 424(6950): 852–855.
17. Arsenault AC, et al. (2006) From colour fingerprinting to the control of photoluminescence in elastic photonic crystals. *Nat Mater* 5(3):179–184.
18. Harun-Ur-Rashid M, Seki T, Takeoka Y (2009) Structural colored gels for tunable soft photonic crystals. *Chem Rec* 9(2):87–105.
19. Kim H, et al. (2009) Structural colour printing using a magnetically tunable and lithographically fixable photonic crystal. *Nat Photonics* 3(9):534–540.
20. Wang C, et al. (2013) User-interactive electronic skin for instantaneous pressure visualization. *Nat Mater* 12(10):899–904.
21. Boer W, Abileah A (2005) US Patent 6,947,102 B2.
22. Choi J, Joo I, Kim H (2010) US Patent 7,800,602 B2.
23. Kreit E, et al. (2012) Biological versus electronic adaptive coloration: How can one inform the other? *J R Soc Interface* 10(78):20120601.
24. Mäthger LM, Hanlon RT (2007) Malleable skin coloration in cephalopods: Selective reflectance, transmission and absorbance of light by chromatophores and iridophores. *Cell Tissue Res* 329(1):179–186.
25. Mathger LM, et al. (2013) Bright white scattering from protein spheres in color changing, flexible cuttlefish skin. *Adv Funct Mater* 23(32):3980–3989.
26. Mäthger LM, Roberts SB, Hanlon RT (2010) Evidence for distributed light sensing in the skin of cuttlefish, *Sepia officinalis*. *Biol Lett* 6(5):600–603.
27. Anonymous (2002) *Chemistry and Applications of Leuco Dyes* (Plenum, New York).
28. Siegel AC, Phillips ST, Wiley BJ, Whitesides GM (2009) Thin, lightweight, foldable thermochromic displays on paper. *Lab Chip* 9(19):2775–2781.
29. Yu C, et al. (2014) All-elastomeric, strain-responsive thermochromic color indicators. *Small* 10(7):1266–1271.
30. Forsythe JW, Hanlon RT (1988) Behavior, body patterning and reproductive biology of *Octopus bimaculoides* from California. *Malacologia* 29(1):41–55.
31. Hanlon RT, Messenger JB (1988) Adaptive coloration in young cuttlefish (*Sepia officinalis* l) - the morphology and development of body patterns and their relation to behavior. *Philos Trans R Soc Lond B Biol Sci* 320(1200):437–487.
32. Mäthger LM, et al. (2007) Disruptive coloration elicited on controlled natural substrates in cuttlefish, *Sepia officinalis*. *J Exp Biol* 210(Pt 15):2657–2666.
33. Zylinski S, Osorio D, Shohet AJ (2009) Cuttlefish camouflage: Context-dependent body pattern use during motion. *Proc R Soc B* 276(1675):3963–3969.
34. Allen JJ, Bell GRR, Kuzirian AM, Velankar SS, Hanlon RT (2014) Comparative morphology of changeable skin papillae in octopus and cuttlefish. *J Morphol* 275(4): 371–390.